Assessment of Residual Coronary Stenoses Using ^{99m}Tc-N-NOET Vasodilator Stress Imaging to Evaluate Coronary Flow Reserve Early After Coronary Reperfusion in a Canine Model of Subendocardial Infarction

Kazuya Takehana, George A. Beller, Mirta Ruiz, Frank D. Petruzella, Denny D. Watson, and David K. Glover

Experimental Cardiology Laboratory, Cardiovascular Division, Department of Medicine, University of Virginia, Charlottesville, Virginia

Reperfusion is often incomplete after recanalization therapy because of the presence of residual coronary stenoses. Detecting mild to moderate stenoses requires assessing coronary flow reserve with vasodilator stress. ^{99m}Tc-(*N*-ethoxy-*N*-ethyl-dithiocarbamato)nitrido (N-NOET) is a viability-independent flow tracer and thus may be well suited for assessing coronary flow reserve in the acute phase of reperfusion. **Methods:** Twelve open-chest dogs underwent 60 min of total left anterior descending artery (LAD) occlusion followed by either full reperfusion (group 1; $n = 4$) or reperfusion through a residual critical stenosis (group 2; $n = 8$). ^{99m}Tc-N-NOET was given during peak vasodilator stress 165 min after reperfusion, and initial and 60-min delayed images were acquired. Regional blood flow was assessed with radiolabeled microspheres. **Results:** Infarct size was similar in both groups (9% $\pm$ 2% vs. 8% $\pm$ 2% of left ventricle). Both initial (0.61 $\pm$ 0.02 vs. 0.73 $\pm$ 0.01; $P < 0.01$) and 60-min (0.67 $\pm$ 0.02 vs. 0.80 $\pm$ 0.01; $P < 0.01$) defect count ratios (LAD/left circumflex coronary artery [LCx]) differentiated between the 2 groups, reflecting the greater diminution in coronary flow reserve in group 2 dogs (LAD/LCx flow ratios = 0.37 $\pm$ 0.04 vs. 0.57 $\pm$ 0.09; $P < 0.01$). Interestingly, coronary flow reserve in the reperfused zone of group 1 was diminished despite the absence of a stenosis. Thus, the difference in ^{99m}Tc-N-NOET uptake between the 2 groups was less than expected. **Conclusion:** In this canine myocardial infarction model with some coronary flow reserve preservation, ^{99m}Tc-N-NOET imaging can detect residual coronary stenoses. However, with more prolonged occlusion resulting in more severe endothelial or microvascular dysfunction, it may be difficult to distinguish varying degrees of vessel patency using any coronary flow reserve technique.

Key Words: coronary flow reserve; myocardial infarction; ^{99m}Tc-N-NOET

J Nucl Med 2001; 42:1388–1394

Therapy for acute myocardial infarction has advanced dramatically with early intravenous fibrinolytic therapy. However, reperfusion is often incomplete because of the presence of residual stenoses in the infarct-related artery. This has intensified the desire of clinical cardiologists to obtain accurate and reproducible estimates of regional myocardial perfusion in this setting. Detection of residual stenoses requires the assessment of coronary flow reserve during either pharmacologic or exercise stress. An ideal perfusion tracer in this setting would permit accurate assessment of coronary flow reserve independent of myocardial viability in the reperfused zone.

A new neutral lipophilic myocardial imaging agent, ^{99m}Tc-(*N*-ethoxy-*N*-ethyl-dithiocarbamato)nitrido (N-NOET), shows high myocardial uptake in various animal species and has been proposed for clinical use in the detection of coronary artery disease (*1–3*). In a previous study from our laboratory, we showed that myocardial ^{99m}Tc-N-NOET uptake, like ^{201}Tl, is proportional to myocardial blood flow over a wide range of adenosine-induced hyperemic flow (*4*). In addition, we have also shown that, unlike ^{201}Tl, ^{99m}Tc-N-NOET uptake after 3 h of coronary occlusion and reperfusion is more reflective of reperfusion flow than myocardial viability (*5*). Thus, we hypothesized that these properties of ^{99m}Tc-N-NOET would make it an ideal tracer for assessing coronary flow reserve after myocardial infarction. Accordingly, the objective of this study was to determine whether vasodilator stress ^{99m}Tc-N-NOET imaging might be useful for detection of residual stenoses early after myocardial infarction.

MATERIALS AND METHODS

All experiments were performed with the approval of the University of Virginia animal care and use committee in compliance with the position of the American Heart Association on the use of research animals.

Received Oct. 9, 2000; revision accepted Jan. 8, 2001.

For correspondence or reprints contact: David K. Glover, ME, Cardiovascular Division, Department of Medicine, P.O. Box 800500, Charlottesville, VA 22908-0500.

Surgical Preparation

Twelve adult mongrel dogs (mean weight, 28.3 ± 0.6 kg), that were subjected to fasting, were anesthetized with sodium pentobarbital (30 mg/kg intravenously), tracheally intubated, and mechanically ventilated with room air (Harvard Apparatus, South Natik, MA) with a positive end-expiratory pressure of 5 cm H_2O. Arterial blood gases were monitored (ABL5; Radiometer America, Westlake, OH) and maintained in the normal physiologic range. The left femoral vein was cannulated with an 8-French catheter for the administration of fluids, sodium pentobarbital, and ^{99m}Tc-N-NOET. Both femoral arteries were cannulated with 8-French catheters and used for microsphere reference blood withdrawal. An additional 7-French catheter was placed in the right femoral artery for arterial pressure monitoring. A 7-French Millar high-fidelity pressure catheter (Millar Instruments, Inc., Houston, TX) was inserted into the left ventricle through an 8-French sheath in the left carotid artery. The left external jugular vein was cannulated with an 8-French catheter for administration of an adenosine A_{2A} receptor agonist, ATL-146e (Adenosine Therapeutics, LLC, Charlottesville, VA).

A left lateral thoracotomy was performed at the level of the fifth intercostal space, and the heart was suspended in a pericardial cradle. A flare-tipped catheter was inserted into the left atrium for pressure measurement and for the injection of radiolabeled microspheres. Two snare ligatures were placed loosely on a proximal portion of the left anterior descending coronary artery (LAD). Ultrasonic flow probes (T206; Transonic Systems, Inc., Ithaca, NY) were placed on a more distal portion of the LAD and left circumflex coronary artery (LCx). Two Doppler sonomicrometer crystals (Crystal Biotech, Holliston, MA) were sutured to the epicardial surface of the heart in the regions supplied by the LAD and LCx to measure regional wall thickening. Throughout each protocol, the electrocardiogram, arterial and left atrial pressures, LAD and LCx flows, and left ventricular pressure and its first time derivative (dP/dt) were continuously monitored and recorded on a 16-channel strip-chart recorder (K2-G; Astro-Med, Inc., West Warwick, RI).

Experimental Protocol

The protocol is shown schematically in Figure 1. Before the setting of the LAD occlusion, baseline recordings were made of heart rate, arterial and atrial pressures, systolic wall thickening, and LAD and LCx flows. A radiolabeled microsphere was injected to measure baseline flow. In 8 of 12 dogs, the first snare was tightened to produce a critical LAD stenosis (group 2). A critical stenosis was defined as the point where baseline flow was unchanged but the reactive hyperemic response to a 10-s total occlusion was completely abolished (*6*). In the other 4 dogs, there was no stenosis (group 1). Next, the second snare ligature was then tightened to produce a complete LAD occlusion for 60 min in both groups of dogs. At the end of the occlusion period, a second set of microspheres was administered. The second snare occluder was then removed in both groups of dogs, allowing full reperfusion in group 1 dogs and partial reperfusion through the residual critical stenosis in group 2 dogs. An intravenous infusion of ATL-146e, a potent and highly selective adenosine A_{2A} receptor agonist (*7*) with potent vasodilator properties, was begun at 165 min after reperfusion at a rate of 0.30 μg/kg/min and continued until the normal zone LCx flow was maximal. This dose of ATL-146e was chosen to produce high coronary flow without decreasing systemic arterial pressure below 85 mm Hg (*8*). When LCx flow was maximal, 296 MBq (8 mCi) ^{99m}Tc-N-NOET were injected into the femoral vein catheter and a third set of microspheres was injected simultaneously into the left atrium. In vivo images were acquired at 5 min and 60 min later. Before the dogs were killed with an overdose of sodium pentobarbital and potassium chloride, the LAD was totally reoccluded with a snare, and 20 mL monastral blue dye were rapidly injected into the left atrial catheter to delineate the anatomic risk area.

Preparation and Quality Control of ^{99m}Tc-N-NOET

^{99m}Tc-N-NOET kits were obtained from CIS-Bio International (Gif sur Yvette, France). Sodium ^{99m}Tc-pertechnetate (740 MBq [20 mCi]) was introduced into a vial containing tin chloride dihydrate (0.100 mg), 1,2-diaminopropane-*N*,*N*,*N*′,*N*′-tetraacetic acid (5.00 mg), succinyl dihydrazide (5.00 mg), and sodium phosphate buffer (pH 7.8). After 15 min at room temperature, 1 mL of a solution containing *N*-ethoxy-*N*-ethyl-dithiocarbamate of sodium monohydrate (10.0 mg/mL) and 1 mL of a solution of dimethyl-β-cyclodextrin (10.0 mg/mL) were added to the first vial. Ten minutes later, ^{99m}Tc-N-NOET was ready to be injected. Quality control was performed with thin-layer chromatography using Silicagel plates (Gelman Sciences, Ann Arbor, MI) and dichloromethane. Radiochemical purity was >90% in each experiment.

Determination of Regional Systolic Thickening

Regional systolic thickening was measured by the epicardial crystal pulsed-Doppler technique (*9*,*10*). This technique is atraumatic, has been validated previously in the canine model, and has been used extensively by our group (*11*). Myocardial systolic

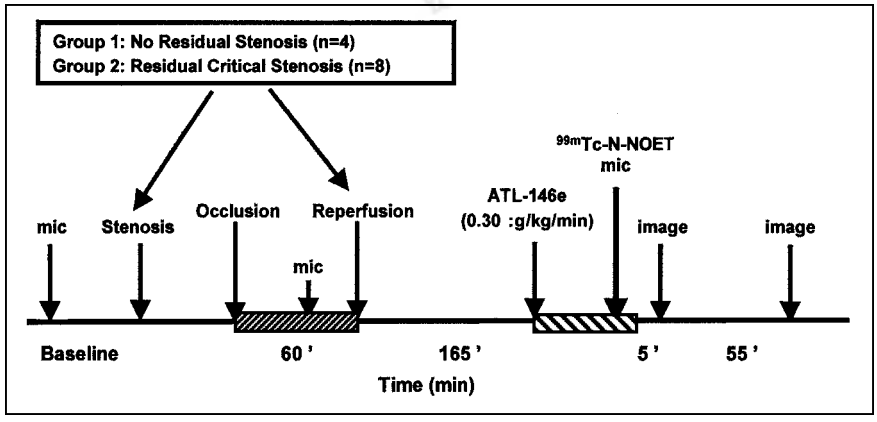

FIGURE 1. Experimental protocol. mic = radiolabeled microspheres.

thickening was measured as the net increase in wall thickness from the onset to the end of systole, as defined by the initial upward stroke of left ventricular pressure and the peak negative deflection of dP/dt, respectively. Systolic thickening was calculated as follows: ([end-systolic thickness − end-diastolic thickness] divided by end-diastolic thickness) × 100%. Measurements of thickening were made over at least 1 respiratory cycle during the last minute of each stage of the protocol, and the highest measured values were reported (excluding beats that followed ventricular ectopy).

Postmortem Analysis

At the end of each protocol, the heart was immediately excised and sliced into 4 approximately 1.5-cm-thick rings from apex to base. The left ventricle and septum were then separated from the remainder of the heart and photographed. Each slice was then carefully traced onto acetate sheets to define the endocardial and epicardial borders and the area at risk. Slices were subsequently incubated in 1% phosphate-buffered triphenyltetrazolium chloride (TTC) solution at 37°C for 10 min to define infarct size, then rephotographed, and retraced on the same acetate sheets. Risk area and infarct area were determined using a digital planimeter program (DigiPlan; Scientific Computing Solutions, LLC, Charlottesville, VA) (*5*).

Image Acquisition and Quantification of Defect Count Ratio

Left lateral planar images were obtained at 5 and 60 min after ^{99m}Tc-N-NOET injection with a standard nuclear medicine gamma camera and computer (Technicare 420; Ohio Nuclear, Solon, OH) with an all-purpose, low- to medium-energy collimator with a 20% window centered around the ^{99m}Tc-N-NOET photopeak and recorded with a 128 × 128 matrix for 4 min (*3*). A lead shield was placed over the abdomen to reduce liver and splanchnic activity. Image quantification and background subtraction were performed on a nuclear medicine computer (Sopha Medical Systems, Buc, France). Ex vivo imaging of heart slices was performed directly on the collimator of the gamma camera for maximal count time (1,638 s) before TTC staining. Quantification of ^{99m}Tc activity was performed on the 2 center slices because the basal slice was above the occlusion and, therefore, always normal, whereas the apical slice lacked a quantifiable normal region. Regions of interest (ROIs) were drawn on the anteroseptal area to represent the infarct zone and on the normal posterior area. The infarct-to-normal count ratio (defect magnitude) was calculated by dividing the counts per pixel in the infarct ROI by the counts per pixel in the normal ROI.

Determination of Regional Myocardial Blood Flow and ^{99m}Tc-N-NOET Activity

The microsphere technique used in our laboratory has been described (*12*). To measure regional tracer activity and microsphere-determined blood flow, each of the 4 heart slices was divided into 6 transmural sections, which were then subdivided into epicardial, midwall, and endocardial segments. The resulting 72 myocardial tissue samples were counted in a γ-well scintillation counter (MINAXI 5550; Packard Instrument Co., Downers Grove, IL) with standard window settings for ^{99m}Tc (120–160 keV) and 3 microspheres (^{113}Sn, 340–440 keV; ^{85}Sr, 450–580 keV; ^{95}Nb, 640–840 keV; or ^{46}Sc, 842–1300 keV). The tissue counts were corrected for background, decay, and isotope spillover, and regional myocardial blood flow was calculated with specialized computer software (PCGERDA; Scientific Computing Solutions). Blood flow and ^{99m}Tc-N-NOET activity for each of the 24 transmural sections were calculated as the weighted average of the 3 corresponding epicardial, midwall, and endocardial segments. Each segment was grouped according to the flow reduction observed during the occlusion period. Segments with endocardial flow during the occlusion period <0.5 mL/min/g were classified as infarct zone and ≥0.5 mL/min/g as normal zone.

Data and Statistical Analysis

All statistical computations were made using SYSTAT software (SPSS, Inc., Chicago, IL). The results are expressed as the mean ± SEM. Differences between means within a group were assessed using repeated-measures ANOVA or a paired *t* test where appropriate, with $P < 0.05$ considered significant. Differences between the 2 groups were assessed using a 1-way ANOVA.

RESULTS

Hemodynamics

Table 1 shows the mean heart rate, systemic arterial pressure, left atrial pressure, maximum positive dP/dt, and LAD and LCx ultrasonic flows at baseline, after setting the critical stenosis (group 2 only), during occlusion, 165 min after reperfusion, and at the peak ATL-146e effect when the tracer was administered. Heart rate and systemic arterial pressure did not change with LAD occlusion and reperfusion. Left atrial pressure increased slightly during occlusion but decreased after reperfusion. Regional systolic wall thickening in the central LAD region decreased significantly ($P < 0.01$) during occlusion and remained akinetic after reperfusion in both groups of dogs. During ATL-146e infusion, mean LCx ultrasonic flow increased significantly in both groups of dogs. Although mean LAD ultrasonic flow in group 1 dogs without a residual stenosis increased significantly compared with that at baseline, the magnitude of the flow increase was blunted significantly compared with the normal zone LCx flow. On the other hand, mean LAD ultrasonic flow in group 2 dogs did not increase during ATL-146e infusion, reflecting the presence of the residual flow-limiting LAD stenosis. Systemic arterial pressure in both groups of dogs decreased slightly but significantly during ATL-146e stress (from 94 ± 2 to 87 ± 2 in group 1, $P < 0.05$; from 96 ± 3 to 89 ± 3 in group 2, $P < 0.01$), and there were reflex rises in heart rate (from 104 ± 7 to 126 ± 5, $P < 0.05$; from 119 ± 5 to 126 ± 5; $P < 0.01$, respectively).

Risk Area and Infarct Size

The risk area (monastral blue dye–negative area) was 30% ± 2% of the left ventricle in group 1 dogs and 27% ± 1% in group 2 dogs. By TTC staining, 9% ± 2% of left ventricle (26% ± 6% of risk area) was infarcted in group 1 and 8% ± 2% (25% ± 5% of risk area) in group 2 dogs. No statistical difference was found in the risk area or infarct size between the 2 groups of dogs.

Regional Myocardial Blood Flow

Table 2 summarizes the mean microsphere-determined regional myocardial blood flows (mL/min/g) in the LAD

TABLE 1
Hemodynamic Parameters

Parameter	Baseline	Stenosis	Occlusion	Reperfusion	Peak ATL-146e
Group 1 (no residual stenosis; $n = 4$)					
Heart rate (bpm)	118 ± 8	—	116 ± 9	104 ± 7	126 ± 5*
MAP (mm Hg)	89 ± 2	—	89 ± 3	94 ± 2	87 ± 2*
LAP (mm Hg)	6 ± 0	—	8 ± 0	7 ± 1	7 ± 0
dP/dt (mm Hg/s)	1,858 ± 80	—	1,682 ± 107	1,675 ± 112	2,448 ± 60†
LAD flow (mL/min)	30 ± 4	—	0 ± 0†	27 ± 4	62 ± 6‡
LAD wall thickening (%)	26 ± 4	—	−6 ± 2†	−7 ± 1†	−1 ± 3†
LCx flow (mL/min)	33 ± 5	—	37 ± 6	23 ± 2	100 ± 21‡
Group 2 (residual critical stenosis; $n = 8$)					
Heart rate (bpm)	124 ± 6	119 ± 6	128 ± 5	119 ± 5	126 ± 5‡
MAP (mm Hg)	94 ± 3	93 ± 4	92 ± 3	96 ± 3	89 ± 3‡
LAP (mm Hg)	7 ± 0	7 ± 0	8 ± 1	7 ± 1	8 ± 1
dP/dt (mm Hg/s)	1,847 ± 70	1,840 ± 91	1,866 ± 73	1,746 ± 52	2,272 ± 83†
LAD flow (mL/min)	26 ± 3	25 ± 5	0 ± 0†	17 ± 2	20 ± 2
LAD wall thickening (%)	24 ± 2	21 ± 3	−8 ± 1†	−7 ± 1†	−4 ± 1†
LCx flow (mL/min)	34 ± 4	33 ± 5	36 ± 5	32 ± 4	102 ± 14‡

*$P < 0.05$ vs. reperfusion.
†$P < 0.01$ vs. baseline.
‡$P < 0.01$ vs. reperfusion.
Reperfusion = 165 min after reperfusion; MAP = mean arterial pressure; LAP = left atrial pressure; dP/dt = peak-positive first derivative of left ventricular pressure with respect to time.
Values are expressed as mean ± SEM.

and LCx zones. After setting the occlusion, myocardial flow in the LAD zone was reduced significantly. No significant difference was found in the magnitude of the flow reduction during occlusion between the 2 groups. During ATL-146e stress, normal coronary flow reserve was observed in the LCx zone in both groups of dogs with a nearly 3-fold flow increase in flow. In group 2 dogs, regional myocardial blood flow in the LAD zone did not increase during ATL-146e infusion because of the presence of the residual LAD critical stenosis. Interestingly, in group 1 dogs, endocardial flow in the LAD zone did not increase during ATL-146e infusion, despite the fact that the LAD was fully reperfused. Moreover, although regional myocardial blood flow in epicardial and midwall segments of group 1 dogs increased compared with baseline flow, these flows were attenuated significantly compared with normal LCx zone flows.

Comparison Between Myocardial ^{99m}Tc-N-NOET Activity Ratio and Blood Flow Ratio

Figure 2 compares the mean LAD/LCx defect count ratios obtained from quantification of background-subtracted in vivo ^{99m}Tc-N-NOET images. For comparison, the trans-

TABLE 2
Regional Myocardial Blood Flows

Myocardial blood flow (mL/min/g)	LAD			LCx		
	Baseline	Occlusion	ATL-146e	Baseline	Occlusion	ATL-146e
Group 1 (no residual stenosis; $n = 4$)						
Epicardium	0.87 ± 0.09	0.28 ± 0.07*	1.68 ± 0.27*	0.87 ± 0.13	0.85 ± 0.12	2.84 ± 0.55*†
Midwall	0.80 ± 0.11	0.18 ± 0.03*	1.33 ± 0.22*	0.90 ± 0.13	0.87 ± 0.12	2.68 ± 0.54*†
Endocardium	0.82 ± 0.12	0.15 ± 0.02*	1.10 ± 0.15	0.93 ± 0.14	0.97 ± 0.17	2.12 ± 0.47*†
Transmural	0.83 ± 0.10	0.20 ± 0.04*	1.38 ± 0.20*	0.90 ± 0.13	0.89 ± 0.13	2.58 ± 0.49*†
Group 2 (residual critical stenosis; $n = 8$)						
Epicardium	0.95 ± 0.10	0.22 ± 0.04*	1.27 ± 0.16*	0.95 ± 0.09	0.87 ± 0.06	2.87 ± 0.25*†
Midwall	0.84 ± 0.07	0.16 ± 0.02*	1.03 ± 0.10	0.95 ± 0.08	0.87 ± 0.06	2.90 ± 0.19*†
Endocardium	0.89 ± 0.08	0.13 ± 0.01*	0.73 ± 0.08	1.02 ± 0.09	0.95 ± 0.08	2.63 ± 0.22*†
Transmural	0.89 ± 0.08	0.17 ± 0.02*	1.02 ± 0.10	0.97 ± 0.08	0.89 ± 0.06	2.82 ± 0.17*†

*$P < 0.02$ vs. baseline.
†$P < 0.05$ vs. LAD.
Values are expressed as mean ± SEM.

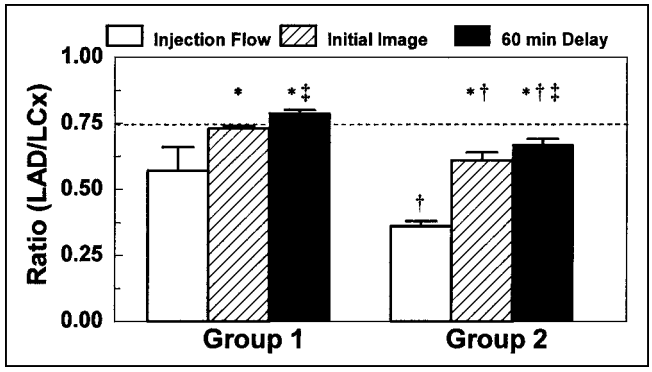

FIGURE 2. Comparison of mean LAD/LCx defect count ratio obtained from background-subtracted in vivo images. Transmural myocardial blood flow ratio at time when ^{99m}Tc-N-NOET was administered during vasodilator stress is superimposed for comparison. Note that initial and 60-min delayed defect count ratios were significantly less in group 2 dogs with residual stenoses than those in group 1 dogs with no stenoses, reflecting greater diminution in coronary flow reserve preserved in group 2 dogs. *$P < 0.05$ vs. injection flow ratio; †$P < 0.01$ vs. group 1; ‡$P < 0.05$ vs. initial image.

mural LAD/LCx myocardial flow ratios at the time when ^{99m}Tc-N-NOET was injected during vasodilator stress are also shown. The initial (0.61 ± 0.02 vs. 0.73 ± 0.01; $P < 0.01$) and 60-min (0.67 ± 0.02 vs. 0.80 ± 0.01; $P < 0.01$) defect count ratios were significantly greater in group 2 dogs with residual critical stenoses than in group 1 dogs with patent vessels, reflecting the greater diminution in coronary flow reserve in group 2 dogs (LAD/LCx flow ratios = 0.37 ± 0.04 vs. 0.57 ± 0.09; $P < 0.01$). In addition, a significant increase in the ^{99m}Tc-N-NOET uptake ratio was found on 60-min images compared with initial (5 min) images in both groups, reflecting some redistribution of ^{99m}Tc-N-NOET.

Figure 3 compares the mean ^{99m}Tc-N-NOET defect count ratios obtained from ex vivo images and the in vitro activity ratios obtained from γ-well counting with the microsphere-determined flow ratio at the time of tracer injection. The mean ^{99m}Tc-N-NOET defect count ratio from the ex vivo images was significantly lower (larger defect) in the group 2 versus group 1 dogs (0.70 ± 0.03 vs. 0.80 ± 0.02; $P < 0.01$). Likewise, the in vitro activity ratio from γ-well counting of myocardial samples was significantly less in the group 2 dogs (0.67 ± 0.05 vs. 0.83 ± 0.06; $P < 0.01$). However, the myocardial uptake ratio of ^{99m}Tc-N-NOET underestimated the LAD/LCx coronary flow ratio at the time when ^{99m}Tc-N-NOET was injected in both groups of dogs, as evidenced by the fact that the ^{99m}Tc-N-NOET activity ratios were significantly greater than the actual flow ratios at the time of tracer injection in both group 1 (0.37) and group 2 (0.57) dogs. Nevertheless, vasodilator stress ^{99m}Tc-N-NOET imaging identified the presence of a residual critical stenosis that reduced the response to vasodilatation.

DISCUSSION

With the advent of reperfusion strategies aimed at restoring coronary patency and improving myocardial blood flow in acute myocardial infarction, the noninvasive assessment of myocardial perfusion has become increasingly important. In addition, measurement of coronary flow reserve has gained wide acceptance as a useful approach in the decision-making process of diagnostic catheterization and coronary intervention. Thus, the assessment of coronary flow reserve can be used not only to diagnose coronary artery disease but also to evaluate the risk of adverse cardiac events and select the most appropriate treatment strategy in patients after acute myocardial infarction.

In a previous study from our laboratory, we examined the usefulness of ^{99m}Tc-sestamibi for assessing coronary flow reserve to identify residual stenoses after reperfusion in a similar canine model (*13*). In dogs with a residual LAD stenosis after reperfusion, ^{99m}Tc-sestamibi activity in the defect region was worse (0.64) than that observed in dogs with a fully patent LAD after reflow (0.72). Nevertheless, the magnitude of the difference in ^{99m}Tc-sestamibi uptake (8%) between the 2 groups of dogs after vasodilator stress was disappointing. Such a small difference in defect magnitude between dogs with and without a severe residual stenosis would be problematic if translated to the clinical setting—that is, with only an average 8% worsening in the tracer uptake ratio in the instance of a residual stenosis versus a totally patent vessel, clearly discriminating between the 2 states could be difficult.

Three possible explanations may be given for why the difference between the 2 groups of dogs was not as striking as expected. First, ^{99m}Tc-sestamibi uptake in the reperfused zone of dogs with a fully patent LAD was diminished because of the presence of subendocardial myocardial infarction (21% of the risk area). Second, there was an un-

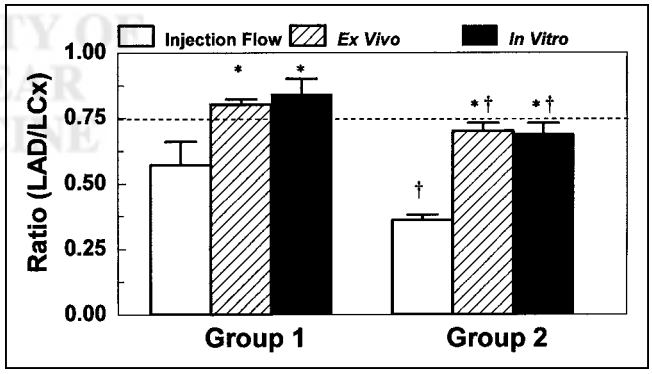

FIGURE 3. Comparison of mean LAD/LCx defect count ratio obtained from ex vivo images and mean LAD/LCx activity count ratio obtained from γ-well counting. For comparison, transmural blood flow ratio is superimposed. LAD/LCx ratios of ex vivo defect and γ-well activity count were less in group 2 dogs than those in group 1 dogs, revealing diminished coronary flow reserve during vasodilator stress in group 2 dogs with critical stenoses. *$P < 0.05$ vs. injection flow ratio; †$P < 0.01$ vs. group 1.

derestimation of the magnitude of the vasodilator-induced ischemia in the group of dogs with residual critical stenoses associated with the plateau in ^{99m}Tc-sestamibi extraction with hyperemia in the normal LCx region. Third, coronary flow reserve in the reperfused zone of the totally reperfused dogs with a patent LAD was attenuated because of endothelial or micovascular dysfunction (or both). The first 2 of these factors result from the biologic properties of ^{99m}Tc-sestamibi—that is, dependence of uptake on myocardial viability and moderate myocardial first-pass extraction, in which ^{99m}Tc-sestamibi uptake fails to track flow in the hyperemic range.

^{99m}Tc-N-NOET, a lipophilic neutral agent, has a high first-pass extraction (0.76) and accurately tracks myocardial blood flow over a relatively wide range. A previous report from our laboratory showed that the myocardial uptake of ^{99m}Tc-N-NOET is closely proportional to blood flow over a wide range of hyperemic flow, with a plateau in uptake seen only at flow rates >3 mL/min/g (*4*). In another study from our laboratory, we showed that ^{99m}Tc-N-NOET uptake after 3 h of occlusion and reperfusion reflects reperfusion flow rather than myocardial viability (*5*). Thus, unlike ^{201}Tl, ^{99m}Tc-sestamibi, or ^{99m}Tc-tetrofosmin, the myocardial uptake of ^{99m}Tc-N-NOET is not dependent on myocardial viability when flow is present; thus, the presence of evolving subendocardial infarction should not significantly impair the uptake of the tracer in reperfused myocardium supplied by a fully patent vessel.

On the basis of these favorable kinetic properties of ^{99m}Tc-N-NOET, we hypothesized that ^{99m}Tc-N-NOET would be better suited than ^{99m}Tc-sestamibi for use as a perfusion tracer for the assessment of coronary flow reserve after reperfusion of an acute myocardial infarction for the detection of a residual coronary stenosis. Indeed, in this study we found that the ^{99m}Tc-N-NOET myocardial activity ratio (LAD/LCx) in the ischemic zone of the group 2 dogs was significantly less than that of the group 1 dogs (0.67 ± 0.05 vs. 0.81 ± 0.07; $P < 0.01$), reflecting the disproportionate flow reserve unmasked by the vasodilator stress. Clinically, this would correspond to a 33% defect versus a 19% defect. The flow ratio of group 2 dogs was 0.36 ± 0.04, a value significantly less than that observed in the group 1 dogs that were fully reperfused (0.53 ± 0.10; $P < 0.01$). In addition, the ^{99m}Tc-N-NOET myocardial activity ratio in the fully reperfused group 1 dogs (0.81) was higher than that observed with ^{99m}Tc-sestamibi (0.72), despite equivalent LAD/LCx flow ratios at the time when the 2 tracers were injected (0.57 vs. 0.56) (*13*). The major reason why the ^{99m}Tc-N-NOET activity ratio was higher than that of ^{99m}Tc-sestamibi is that ^{99m}Tc-N-NOET underwent early redistribution as a result of differential washout during the 60-min period after injection, whereas ^{99m}Tc-sestamibi did not. The quantitative in vivo imaging data from the fully reperfused dogs in both studies showed that over 60 min, the defect count ratio (LAD/LCx) for ^{99m}Tc-N-NOET increased from 0.73 to 0.80, whereas with ^{99m}Tc-sestamibi the defect count ratio remained fixed at 0.71 (*13*). A similar degree of early redistribution was also observed in the group 2 dogs that underwent reperfusion through a residual stenosis (^{99m}Tc-N-NOET defect count ratio increased from 0.61 to 0.67). Rapid, early myocardial ^{99m}Tc-N-NOET redistribution after tracer injection during vasodilator stress has also been reported from our laboratory in a canine model of a critical coronary stenosis (*14*).

Although ^{99m}Tc-N-NOET uptake in the reperfused zone was significantly less in the dogs with severe residual LAD stenoses compared with that of the dogs with fully patent coronary vessels, the difference in ^{99m}Tc-N-NOET defect magnitude between these 2 groups was not as great as we had expected. As observed with ^{99m}Tc-sestamibi (*13*), the difference in myocardial activity was not greater between the 2 groups of dogs mainly because of the less-than-expected tracer uptake in the LAD zone in dogs that were fully reperfused with no residual LAD stenosis. The major limiting factor for ^{99m}Tc-N-NOET uptake in the LAD zone was the marked diminution of coronary flow reserve in this zone. For example, the myocardial blood flow ratio (LAD/LCx) in the group 1 dogs with a fully patent LAD was much less than unity (0.53 ± 0.10). Whereas absolute flow in the LCx increased nearly 3-fold during vasodilator stress compared with that at baseline (from 0.90 ± 0.13 to 2.58 ± 0.49 mL/min/g), coronary flow was markedly attenuated in the fully reperfused LAD zone (from 0.83 ± 0.10 to 1.38 ± 0.20 mL/min/g). Thus, even in the absence of a physical residual coronary stenosis, coronary flow reserve in the reperfused zone was severely diminished in the early phase of coronary reperfusion. We confirmed previously that the attenuation in coronary flow reserve early after reperfusion was caused by endothelial or microvascular damage (or both) by showing marked diminution in the coronary flow responses to postreflow tests of reactive hyperemia as well as intracoronary provocation with adenosine and acetylcholine. (*13*). Therefore, even in the absence of a physical stenosis, a functional stenosis may be present.

The decreased coronary flow reserve in the infarct zone immediately after coronary reperfusion indicates an increase in the passive resistance in the reperfused vascular bed. Leukocyte plugging of the microvasculature in the reperfused myocardium and development of intracellular and interstitial edema may explain the inability of myocardial arterioles to dilate in this setting (*15–18*). The attenuation of endothelium-dependent coronary vasodilator function is also an important predictor of coronary flow reserve after myocardial infarction (*19–21*). In addition, several studies have shown that coronary flow reserve is reduced not only in the ischemic and infarct zones but also in remote regions supplied by angiographically normal coronary arteries (*22–24*). Some studies showed that coronary flow reserve in the infarcted zone was decreased significantly after 2 h of reperfusion but gradually returned to near preocclusion baseline values within 1 wk (*25,26*). Moreover, other investigators have shown that with more pro-

longed occlusion times, the diminution in coronary flow reserve in the occlusion–reperfusion zone may result from more severe endothelial or microvascular dysfunction (*27*,*28*).

CONCLUSION

In this canine model of predominantly subendocardial infarction, very early assessment of coronary flow reserve using vasodilator stress ^{99m}Tc-N-NOET perfusion imaging can detect the presence of a residual coronary stenosis after reperfusion. However, as revealed in this study, a major limitation in being able to distinguish the severity of a residual coronary stenosis using a technique that measures coronary flow reserve early after reperfusion of an acute myocardial infarction is that, even in the absence of a physical coronary stenosis, coronary flow reserve may be severely attenuated or abolished. This limitation applies not only to all nuclear perfusion tracers but also to other techniques based on using coronary flow reserve as a variable, such as gadolinium MRI, enhanced echocardiography, PET, or Doppler wire intracoronary catheters. A second possible limitation is that, even with a fully patent vessel, the severe systolic left ventricular dysfunction (myocardial stunning) that is usually present in this setting will create partial-volume defects on images. Thus, an abnormal scan might be misinterpreted as being indicative of a residual stenosis.

ACKNOWLEDGMENT

The authors thank CIS-Bio International for providing the ^{99m}Tc-N-NOET used in this experimental study.

REFERENCES

1. Ghezzi C, Fagret D, Arvieux CC, et al. Myocardial kinetics of Tc-N-NOET: a neutral lipophilic complex tracer of regional myocardial blood flow. *J Nucl Med*. 1995;36:1069–1077.
2. Fagret D, Marie PY, Brunotte F, et al. Myocardial perfusion imaging with technetium-99m-Tc NOET: comparison with thallium-201 and coronary angiography. *J Nucl Med*. 1995;36:936–943.
3. Vanzetto G, Calnon DA, Ruiz M, et al. Myocardial uptake and redistribution of ^{99m}Tc-N-NOET in dogs with either sustained coronary low flow or transient coronary occlusion: comparison with ^{201}Tl and myocardial blood flow. *Circulation*. 1997;96:2325–2331.
4. Calnon DA, Ruiz M, Vanzetto G, Watson DD, Beller GA, Glover DK. Myocardial uptake of ^{99m}Tc-N-NOET and ^{201}Tl during dobutamine infusion: comparison with adenosine stress. *Circulation*. 1999;100:1653–1659.
5. Vanzetto G, Glover DK, Ruiz M, et al. ^{99m}Tc-N-NOET myocardial uptake reflects myocardial blood flow and not viability in dogs with reperfused acute myocardial infarction. *Circulation*. 2000;101:2424–2430.
6. Glover DK, Ruiz M, Edwards NC, et al. Comparison between ^{201}Tl and ^{99m}Tc sestamibi uptake during adenosine-induced vasodilatation as a function of coronary stenosis severity. *Circulation*. 1995;91:813–820.
7. Okusa MD, Linden J, Macdonald T, Huang L. Selective A_{2A} adenosine receptor activation reduces ischemia-reperfusion injury in rat kidney. *Am J Physiol*. 1999;277:F404–F412.
8. Glover DK, Ruiz M, Takehana K, Petruzella FD, Watson DD, Beller GA. Vasodilator stress imaging using new adenosine A_{2A} receptor agonists administered by bolus injection [abstract]. *J Am Coll Cardiol*. 2000;35:A-492.
9. Hartley CJ, Latson LA, Michael LH, Seidel CL, Lewis RM, Entman ML. Doppler measurement of myocardial thickening with a single epicardial transducer. *Am J Physiol*. 1983;245:H1066–H1072.
10. Zhu WX, Myers ML, Hartley CJ, Roberts R, Bolli R. Validation of a single crystal for measurement of transmural and epicardial thickening. *Am J Physiol*. 1986;251:H1045–H1055.
11. Calnon DA, Glover DK, Beller GA, et al. Effects of dobutamine stress on myocardial blood flow, ^{99m}Tc sestamibi uptake, and systolic wall thickening in the presence of coronary artery stenoses: implications for dobutamine stress testing. *Circulation*. 1997;96:2353–2360.
12. Heymann MA, Payne BD, Hoffman JIE, Rudolph AM. Blood flow measurement with radionuclide-labeled particles. *Prog Cardiovasc Dis*. 1977;20:55–79.
13. Takehana K, Ruiz M, Petruzella FD, Watson DD, Beller GA, Glover DK. Early detection of myocardial viability and ischemia using a dual isotope approach following coronary reperfusion [abstract]. *Circulation*. 1999;100:I-866.
14. Petruzella FD, Ruiz M, Katsiyiannis P, et al. Optimal timing for initial and redistribution ^{99m}Tc-N-NOET image acquisition. *J Nucl Cardiol*. 2000;7:123–131.
15. Humphrey SM, Thomson RW, Gavin JB. The effect of an isovolumic left ventricle on the coronary vascular competence during reflow after global ischemia in the rat heart. *Circ Res*. 1981;49:784–791.
16. Engler RL, Schmid-Schonbein GW, Pavelec RS. Leukocyte capillary plugging in myocardial ischemia and reperfusion in the dogs. *Am J Pathol*. 1983;111:98–111.
17. Powers ER, DiBona DR, Powell WJ Jr. Myocardial cell volume and coronary resistance during diminished coronary perfusion. *Am J Physiol*. 1984;247:H467–H477.
18. Nichols WW, Mehta JL, Donnelly WH, Lawson DL, Thompson LV, ter Riet M. Reduction in coronary vasodilator reserve following coronary occlusion and reperfusion in anesthetized dog: role of endothelial-derived relaxing factor, myocardial neutrophil infiltration and prostaglandins. *J Mol Cell Cardiol*. 1988;20:943–954.
19. Mehta JL, Nichols WW, Donnelly WH, Lawson DL, Saldeen TG. Impaired canine coronary vasodilator response to acetylcholine and bradykinin after occlusion-reperfusion. *Circ Res*. 1989;64:43–54.
20. Quillen JE, Sellke FW, Brooks LA, Harrison DG. Ischemia-reperfusion impairs endothelium-dependent relaxation of coronary microvessels but does not affect large arteries. *Circulation*. 1990;82:586–594.
21. Kloner RA, Giacomelli F, Alker KJ, Hale SL, Matthews R, Bellows S. Influx of neutrophils into the walls of large epicardial coronary arteries in response to ischemia/reperfusion. *Circulation*. 1991;84:1758–1772.
22. Gascho JA, Beller GA. Adverse effects of circumflex coronary artery occlusion on blood flow to remote myocardium supplied by a stenosed left anterior descending coronary artery in anesthetized open-chest dogs. *Am Heart J*. 1987;113:679–683.
23. Uren NG, Crake T, Lefroy DC, de Silva R, Davies GJ, Maseri A. Reduced coronary vasodilator function in infarcted and normal myocardium after myocardial infarction. *N Eng J Med*. 1994;331:222–227.
24. Wu JC, Yun JJ, Dione DP, Heller EN, Deckelbaum LI, Sinusas AJ. Severe regional ischemia alters coronary flow reserve in the remote perfusion area. *J Nucl Cardiol*. 2000;7:43–52.
25. Bloor CM, White FC. Coronary artery reperfusion: effects of occlusion duration on reactive hyperemic responses. *Basic Res Cardiol*. 1975;70:148–158.
26. Vanhaecke J, Flameng W, Borgers M, Jang IK, Van de Werf F, De Geest H. Evidence for decreased coronary flow reserve in viable postischemic myocardium. *Circ Res*. 1990;67:1201–1210.
27. Klein LW, Agarwal JB, Schneider RM, Hermann G, Weintraub WS, Helfant RH. Effects of previous myocardial infarction on measurements of reactive hyperemia and the coronary vascular reserve. *J Am Coll Cardiol*. 1986;8:357–363.
28. Marzullo P, Parodi O, Sambuceti G, et al. Residual coronary reserve identifies segmental viability in patients with wall motion abnormality. *J Am Coll Cardiol*. 1995;26:342–350.

JNM The Journal of NUCLEAR MEDICINE

Assessment of Residual Coronary Stenoses Using ^{99m}Tc-N-NOET Vasodilator Stress Imaging to Evaluate Coronary Flow Reserve Early After Coronary Reperfusion in a Canine Model of Subendocardial Infarction

Kazuya Takehana, George A. Beller, Mirta Ruiz, Frank D. Petruzella, Denny D. Watson and David K. Glover

J Nucl Med. 2001;42:1388-1394.

The Journal of Nuclear Medicine is published monthly.
SNMMI | Society of Nuclear Medicine and Molecular Imaging
1850 Samuel Morse Drive, Reston, VA 20190.
(Print ISSN: 0161-5505, Online ISSN: 2159-662X)

SNMMI SOCIETY OF NUCLEAR MEDICINE AND MOLECULAR IMAGING